XL CILAMCE
IBERO-LATIN AMERICAN CONGRESS ON COMPUTATIONAL METHODS IN ENGINEERING
NOVEMBER 11-14, 2019
Praiamar Natal Hotel & Convention Natal, RN-BRAZIL

A LUMPED DAMAGE MODEL FOR THE ANALYSIS OF DUAL SYSTEMS OF REINFORCED CONCRETE

Julio Neumann
julio.neumann@hotmail.com
Universidade Federal da Integração Latino-Americana
Avenida Silvio Américo Sasdelli, 1842 - Bairro Itaipu A, Edifício Comercial Lorivo. CEP: 85866-000 | Caixa Postal 2044 - Foz do Iguaçu - Paraná.
Ricardo Picón
ricardo.picon@gmail.com
Universidad Católica de Temuco
Rudecindo Ortega 2950, Temuco, Región de Araucanía, Chile.
Julio Flórez López
j.florezlopez@gmail.com
Universidade Federal da Integração Latino-Americana
Avenida Silvio Américo Sasdelli, 1842 - Bairro Itaipu A, Edifício Comercial Lorivo. CEP: 85866-000 | Caixa Postal 2044 - Foz do Iguaçu - Paraná.

Abstract. The search for mathematical models capable of estimating the level of degradation of reinforced concrete structures is increasing. However, due to the complexity, the number of variables involved and the physical non-linearity of the problem, the determination of these models becomes somewhat complicated. Due to this need, there are behavioral models for elements with bending failure and behavioral models for elements with shear failure that have been proposed independently. However, there are still few models that include the evaluation of the inelastic response considering the interaction between the two types of forces (shear force and bending moment). In addition, the models proposed in the literature have as main limitation the uncertainty in the selection of parameters that adequately represent the inelastic behavior of the elements. To overcome these difficulties, in this paper, it is proposed a constitutive model based on lumped damage mechanics (LDM). A finite element is used that includes two auxiliary subroutines capable of representing the inelastic behavior of the structure considering the two types of forces. The model was validated through comparisons of results of numerical simulations with experimental results. Later, the model is used for the dynamic analysis of dual systems. The results show that the proposed model is interesting because besides being able to use to verify the structural integrity of already completed buildings, it can contribute to the realization of more advanced projects, in such a way that the cracking during a loading can be controlled and prevent structural collapse.

Keywords: Reinforced concrete, Dual systems, Plastic hinges, Bending and shear damage.

1 Introduction

The reinforced concrete (RC), while not the only option, is still the most widely used material worldwide for the construction of civil engineering structures (e.g. buildings, bridges, tunnels, containment structures, dams, etc.). Designing RC structures involves the use of codes that are based on certain fundamental principles related to structural safety. The guidelines included in the codes are intended to ensure compliance with the principles for the highest variety of applications. However, codes do not always propose logical procedures (due to the simplifications they contain) to quantify the degree of structural safety of an existing project. Seismic codes correspond to the most representative case of this situation.

It is evident that in recent years, the occurrence of increasingly catastrophic seismic events has evidenced on the importance and the need to evaluate the inelastic behavior of RC structures that could possibly exhibit inappropriate seismic performance.

Seismic codes generally have the following philosophy: Under minor but frequent earthquakes, the main elements of buildings carrying vertical and horizontal forces (e.g. beams, columns, etc.) should not be damaged; however, parts that have no structural function (e.g. masonry walls, etc.) may suffer repairable damage. Under moderate but frequent earthquakes, both may experience repairable damage. Under strong but rare seismic events, main elements can be severely damaged, but the building should not collapse. In fact, the range of practical applications is so wide that standards-based designs do not always comply with the principles of structural security. Other important case that should be considered is the increased seismicity of a given zone as a consequence of human activities (induced seismicity). In these cases, the need to have a tool of diagnosis to quantify the degree of security of structural projects is critical (FLÓREZ-LÓPEZ et. al, 2014 [1]).

To estimate the safety of buildings, mathematical models have been developed to evaluate the inelastic behavior of structures subjected to seismic loads. The efficiency of these models depends on the ability to represent the main effects induced by earthquakes, such as: permanent deformations, decrease in stiffness and resistance, degradation of the material due to fatigue, etc. (PERDOMO et. al, 2013 [2]). There are currently behavioral models for bending failure elements and models for shear failure elements (THOMSON et. al, 2009 [3]). However, there are still few models that include the evaluation of inelastic response considering the interaction between the two types of forces (shear force and bending moment).

The models proposed in the literature present as main limitation the uncertainty in the selection of the parameters that adequately represent the inelastic behavior of the structural elements. In the present paper, is used a finite element capable of representing (in function of the structural configuration, the physical and geometrical characteristics of the material, the nature of the loads and the dispositions of the design codes) the inelastic behavior of the structure considering interaction between the shear forces and bending moments. Unlike the models found in the literature, the model is based on the concepts of lumped damage mechanics, which is a branch of structural mechanics that combines the concepts of fracture mechanics and continuous damage theory with structural analysis procedures.

The model is validated by comparing experimental results with numerical simulations. Subsequently, it is used for the diagnostic of dual systems (frames and shear walls combination). Dual systems are often used as a good structural alternative for buildings and industrial installations in earthquake-prone areas.

2 Model Formulation

2.1 Damage model using internal variables

The formulation of nonlinear behavioral models is based on experimental studies that allow characterizing the dissipation mechanisms of structural elements when subjected to severe overloads (e.g., wind forces, seismic loads, etc.). Experimental results show that the failure mechanisms produced by the shear forces and bending moments can be considered independently, which allows to propose a

model that couples an element with concentrated dissipation at the extremes due to flexion and a dissipation element distributed along full length due to shear.

The model uses the finite element method to perform a numerical approximation transforming the continuous system into discrete. Considering the analysis based on this method, a structure can be represented as a disposition of connected elements capable of stably bearing loads under certain deformations conditions. In each element are defined variables that aim to represent the dissipation mechanisms observed experimentally. To formulate the finite element, it is necessary to define the variables of the inelastic behavior model such as: nodal displacements, generalized deformations, generalized stresses and the internal variables that represent the rigidity degradation and plastic deformations of the element due to bending and the shear.

Consider an RC structure composed of n nodes and m elements of any aspect ratio (for RC elements, the aspect ratio is the ratio between the lateral load application point and the effective cross-section height). One node i has three degrees of freedom: the displacements u_i and w_i in the direction of the global axes X and Y and the rotation θ_i. The generalized deformations of an element b located between nodes i and j are represented by the matrix $\{\Phi\}_b^t = \left(\phi_i^b, \phi_j^b, \delta_b\right)$. The variables ϕ_i^b and ϕ_j^b represent the relative rotations and δ_b is the elongation of the element (see Fig. 2.1a). Generalized stresses are represented by the matrix $\{M\}_b^t = \left(m_i^b, m_j^b, n_b\right)$ which includes the bending moments and the axial force in the element (see Fig. 2.1b).

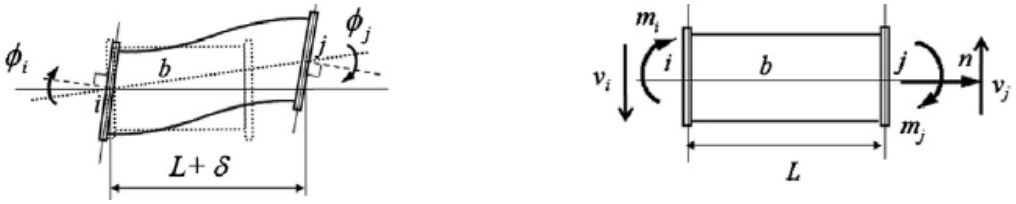

(a) Generalized deformations (b) Generalized stresses

Figure 2.1. Representation of generalized deformations and stresses for an RC element.

If the forces distributed on the element are small relative to the nodal forces, the shear force will be approximately constant and can be calculated as:

$$v_i \cong v_j \cong V_b = \frac{m_i^b + m_j^b}{L_b} \tag{1}$$

Arbitrary aspect ratio RC elements usually present cracks due to bending in the plastic hinge zone and cracks due to shear forces along the length of the element. The simplified representation of the cracking process is obtained using the damage variables shown in Fig. 2.2. These parameters range from zero to one as in continuum damage mechanics, but in this case, they represent macro-cracks densities rather than micro-defects.

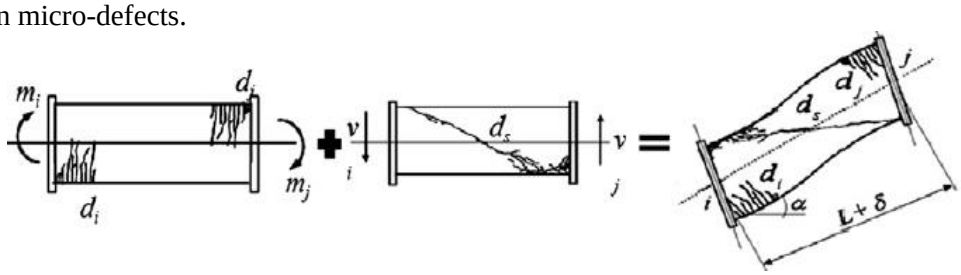

Figure 2.2. Representation of internal variables for an RC element.

The damage due to bending is concentrated on the plastic hinges and can be represented by the matrix $(D)_b = \left(d_i, d_j\right)$. The particularity of this model is that it proposes the introduction of a new internal damage variable d_s that is responsible for quantifying the damage due to shear forces.

According to Thomson et. al, (2009) [3], there are two main sources of possible plastic deformations of the RC elements. The first is related to the longitudinal reinforcement yield. Conventionally, these plastic deformations are represented as rotations of the plastic hinges that can be grouped into the generalized plastic deformation matrix $\{\Phi^p\}_b^t = \left(\phi_i^p, \phi_j^p, 0\right)$, in which case the elongation permanent is neglected. The second mechanism is related to the yield of the transverse

reinforcement that produces plastic distortions of the element and can be represented by the plastic distortion matrix $\{\gamma^p\}_b^t = (\gamma^p, \gamma^p, 0)$. The physical interpretation of each variable show in Fig. 2.3.

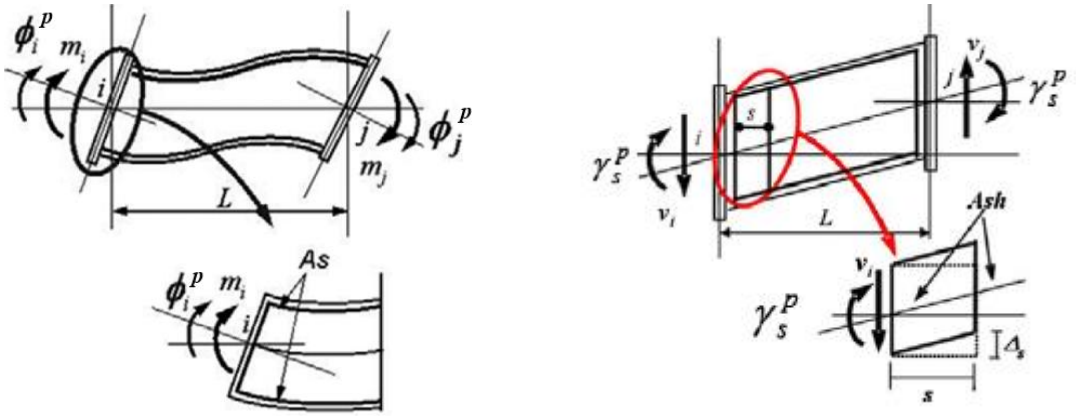

(a) Plastic deformations (b) Plastic distortions

Figure 2.3. Plastic deformations and plastic distortions for an RC element.

2.2 Constitutive equations

The constitutive laws of continuous damage mechanics are based on two important concepts: the effective stress and the deformation equivalence hypothesis (LEMAITRE; CHABOCHE, 1998 [4]):

$$\bar{\sigma} = \frac{\sigma}{1-\omega}; \qquad \bar{\sigma} = E(\varepsilon - \varepsilon^p) \;\Rightarrow\; \sigma = (1-\omega)(\varepsilon - \varepsilon^p) \tag{2}$$

where ω is the continuous damage variable, having values between zero and one. Instead of writing the law of state in terms of rigidity as in Eq. (2), it is better for the purpose of this document to express it in terms of flexibility:

$$\varepsilon - \varepsilon^p = \frac{\sigma}{(1-\omega)E} \;\Rightarrow\; \varepsilon = \varepsilon^e + \varepsilon^d + \varepsilon^p \qquad \varepsilon^e = \frac{\sigma}{E} \qquad \varepsilon^d = \frac{\omega\sigma}{(1-\omega)E} \tag{3}$$

Note that the term ε^e corresponds to an elastic strain, ε^p is the plastic strain, and ε^d can be interpreted as an additional strain produced by the damage variable. If the continuous damage variable is zero, the additional deformation ε^d is also zero. If damage tends to one, the additional deformation associated with damage tends to infinite. Note in Eq. (3) the existence of three deformation terms for the three phenomena considered: elasticity, damage and plasticity.

For the case of RC elements, five main phenomena are identified. Thus, according to the hypothesis of deformation equivalence, the total deformation is decomposed into five terms: an elastic deformation, a distortion term due to the damage produced by the shear force, a deformation term due to the damage produced by the bending moment, the plastic distortion matrix and the plastic rotation matrix.

$$\{\Phi\}_b = \{\Phi^e\}_b + \{\gamma^d\}_b + \{\Phi^d\}_b + \{\gamma^p\}_b + \{\Phi^p\}_b \tag{4}$$

The elastic deformation, which corresponds to the first term of Eq. (4), can be written as a function of stress using conventional flexibility matrices:

$$\{\Phi^e\}_b = [F_0]_b\{M\}_b; \qquad [F_0]_b = \begin{bmatrix} \frac{L_b}{3EI_b} & -\frac{L_b}{6EI_b} & 0 \\ -\frac{L_b}{6EI_b} & \frac{L_b}{3EI_b} & 0 \\ 0 & 0 & \frac{L_b}{EA_b} \end{bmatrix} + \begin{bmatrix} \frac{1}{GA_bL_b} & \frac{1}{GA_bL_b} & 0 \\ \frac{1}{GA_bL_b} & \frac{1}{GA_bL_b} & 0 \\ 0 & 0 & 0 \end{bmatrix} \tag{5}$$

The first part of $[F_0]_b$ corresponds to Bernoulli elastic flexibility matrix and the second term is Timoshenko elastic flexibility matrix. Parameters EI_b and GA_b correspond to flexural and shear rigidities, respectively. The additional distortions produced by the increase in shear damage, corresponding to the second term of Eq. (4), can be written according to the hypothesis of deformation equivalence, such as:

$$\{\gamma^d\}_b = [C_s(d_s)]_b\{M\}_b; \qquad [C_s(d_s)]_b = \frac{d_s}{1-d_s}\begin{bmatrix} \frac{1}{GA_bL_b} & \frac{1}{GA_bL_b} & 0 \\ \frac{1}{GA_bL_b} & \frac{1}{GA_bL_b} & 0 \\ 0 & 0 & 0 \end{bmatrix} \tag{6}$$

Note that if damage due to shear force is zero, the additional distortion produced by damage is also zero. If shear damage tends to one, Timoshenko flexibility tends to infinity. Similarly, the third term of Eq. (4) is given by:

$$\{\Phi^d\}_b = \left[C_f(D)\right]_b\{M\}_b; \qquad \left[C_f(D)\right]_b = \begin{bmatrix} \frac{d_i}{1-d_i}\frac{L_b}{3EI_b} & 0 & 0 \\ 0 & \frac{d_j}{1-d_j}\frac{L_b}{3EI_b} & 0 \\ 0 & 0 & 0 \end{bmatrix} \tag{7}$$

Bernoulli terms of flexibility tend to infinity when due flexural damage tends to one. The combination of Eq. (4) and (7) provides the state law for an RC element:

$$\{\Phi - \Phi^p - \gamma^p\}_b = [F(D,d_s)]\{M\}_b$$

$$[F(D,d_s)] = \begin{bmatrix} \frac{L_b}{3EI_b(1-d_i)} + \frac{1}{GA_bL_b(1-d_s)} & -\frac{L_b}{6EI_b} + \frac{1}{GA_bL_b(1-d_s)} & 0 \\ -\frac{L_b}{6EI_b} + \frac{1}{GA_bL_b(1-d_s)} & \frac{L_b}{3EI_b(1-d_j)} + \frac{1}{GA_bL_b(1-d_s)} & 0 \\ 0 & 0 & 0 \end{bmatrix} \tag{8}$$

The local stiffness matrix is of course the inverse of $[F(D,d_s)]$ and its computation is immediate when any symbolic manipulation program is used, but the resulting expression is too complex to be read and interpreted easily.

2.3 Generalized criterion of Griffith

The theory of linear elastic fracture mechanics states that crack propagation is only possible if the energy stored in the structure is sufficient to overcome the crack resistance of the material. The same energy balance of Griffith can be used in this case. The complementary strain energy W_b of an RC element can be calculated from state law.

$$W_b = \frac{1}{2}\{M\}_b^t\{\Phi - \Phi^p - \gamma^p\}_b = \frac{1}{2}\{M\}_b^t[F(D,d_s)]_b\{M\}_b \tag{9}$$

Assuming that the mechanisms of damage due to shear forces and bending moments occur independently, the energy release rate for shear damage G_s is given by:

$$G_s = \frac{\partial W_b}{\partial d_s} = \frac{L_b {V_b}^2}{2GA_b(1-d_s)^2} \tag{10}$$

Note that this variable depends on the shear force V_b. The use of Griffith generalized criterion also allows the calculation of the shear damage variable:

$$\begin{cases} \Delta d_s = 0 & if \quad G_s < R_s \\ G_s = R_s & if \quad \Delta d_s > 0 \end{cases} \tag{11}$$

where R_s is the shear damage resistance function that can be experimentally identified (see PERDOMO et. al, 2013 [2]) and Δd_s represents the shear damage increments. This generalized form of Griffith criterion was also discussed by Thomson et. al, (2009) [3].

If we consider a cantilever RC shear wall subjected to a monotonic charge, the state law described in Eq. (8) becomes:

$$V = Z(d_s)\left(t - t_p\right); \qquad t_p = \gamma^p L; \qquad Z(d_s) = \frac{3EIGA(1-d_s)}{L(L^2GA - L^2GAd_s + 3EI)} \tag{12}$$

where t is the displacement and V is the force. The values of Z may be measured in the test. Thus, an experimental value of shear damage can be determined for each discharge performed in the test using the following equation:

$$d_s = \frac{3EIGA - 3ZLEI - ZL^3GA}{GA(3EI - L^3Z)} \tag{13}$$

Note that Eq. (13) is simply an extension of the method of varying elastic rigidity of fracture mechanics and continuous damage (LEMAITRE; CHABOCHE, 1998 [4]). It is possible to construct a shear damage curve against the shear energy release rate (Fig. 2.4b), because the experimental values of the latter variables can be obtained using Eq. (10). With this graph, it is possible to propose the following expression for the shear damage resistance function:

$$R(d_s) = R_{0s} + q_s \frac{\ln(1 - d_s)}{1 - d_s} \tag{14}$$

There is an initial value of shear strength R_{0s} and a logarithmic hardening term. The latter is due to the action of the reinforcement that prevents the propagation of shear cracks. In practical applications, the parameters R_{0s} and q_s need not be measured experimentally; they can be determined from concepts of the theory of reinforced concrete, as explained below.

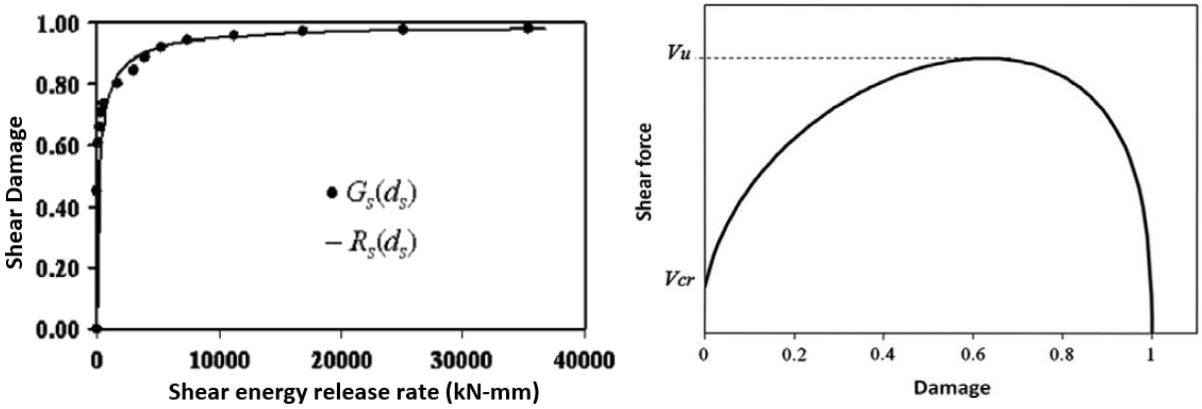

(a) Shear energy release rate vs. Damage (b) Damage vs. Shear force

Figure 2.4. Energy release rate according to generalized Griffith criterion.

Consider again the Griffith equation: $G_s = R_s$. This expression defines a general relationship between shear force and shear damage (see Eq. (15) and Fig. 2.4b):

$$L_b {V_b}^2 = 2GA_b(1 - d_s)^2 \left(R_{0s} + q_s \frac{\ln(1 - d_s)}{1 - d_s}\right) \tag{15}$$

Note that the values of cracking force V_{cr} and the values of ultimate shear force V_u can be calculated using the reinforced concrete theory with reasonable accuracy (ACI, 2005 [5]; SEZEN; MOEHLE, 2004 [6]). These values allow the calculation of the parameters R_{0s} and q_s using the shear strength function. Bending damage can also be calculated using the same procedure:

$$G_i = \frac{\partial W_b}{\partial d_i} = \frac{L_b {m_i}^2}{6EI_b(1 - d_i)^2}; \qquad G_j = \frac{\partial W_b}{\partial d_j} = \frac{L_b {m_j}^2}{6EI_b\left(1 - d_j\right)^2} \tag{16}$$

Note that these new energy release rates now depend on bending moments rather than shear force. Similar generalized forms of Griffith's criterion can also be proposed and the corresponding bending strength function identified (CIPOLLINA et. al, 1995 [7]). The same method of varying elastic rigidity can also be adapted for the experimental measurement of bending damage. It is interesting to note that the bending damage resistance function of a plastic hinge i may have the same general expression as Eq. (14) but of course with different values for the parameters:

$$R(d_i) = R_{0f} + q_f \frac{\ln(1 - d_i)}{1 - d_i} \tag{17}$$

2.4 Yield functions

The last components of the model are the yields functions necessary for the calculation of plastic distortions and plastic rotations. First, we use the conventional yield functions with linear kinematic hardening; then the deformation equivalence hypothesis is used considering the effective shear force

and effective bending moment.

$$\bar{V} = \frac{V}{1-d_s} = \frac{m_i + m_j}{(1-d_s)L}; \qquad \overline{m_i} = \frac{m_i}{1-d_i} \tag{18}$$

$$f_s = |\bar{V} - c_s\gamma^p| - k_{0s} = \left|\frac{m_i + m_j}{(1-d_s)L} - c_s\gamma^p\right| - k_{0s} \leq 0; \tag{19}$$

$$f_i = \left|\frac{m_i}{1-d_i} - c_i\phi_i^p\right| - k_{0i} \leq 0 \tag{20}$$

where c_s, c_i, k_{0i} and k_{0s} are also model parameters. All of them can also be calculated using reinforced concrete theory (PERDOMO, 2010 [8]). The last expressions for a complete analysis of reinforced concrete structures are the kinematic and equilibrium equations. Both are exactly the same as in inelastic frame analysis.

2.5 Unilateral damage

During cyclic loadings, two distinct sets of cracks appear on opposite faces of the elements. One due to positive moments or shear forces, another for negative actions. With the reversal of the forces, the cracks that were created by the loading close and cease to have influence in the behavior of the element. This effect is called "unilateral damage" in the literature. The simplest way to describe unilateral effects consists in introducing two sets of damage variables denoted $(D^+)_b = (d_i^+, d_j^+)$, d_s^+ and $(D^-)_b = (d_i^-, d_j^-)$, d_s^-. They describe cracking due to respectively, positive and negative actions (see Fig 2.5) (MAZARS et. al, 1990 [11]; LADEVÈZE, 1991 [12]). Each set of damage are computed using independent Griffith criteria as indicated in section 2.2. The numerical simulations presented in the next section were carried out considering the unilateral effects.

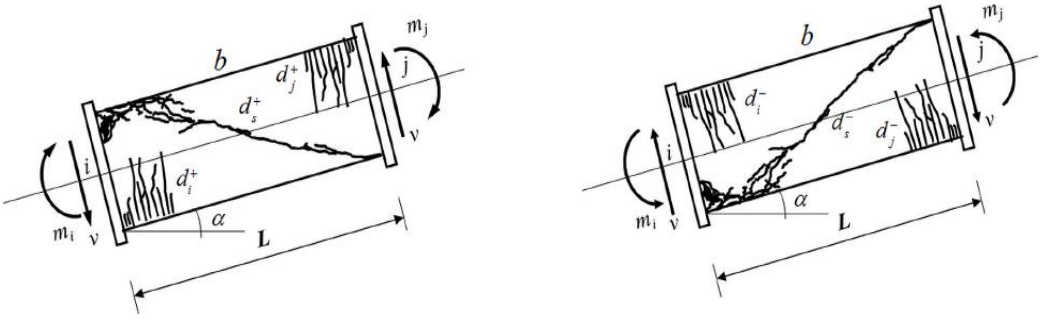

(a) Positive damages (b) Negative damages

Figure 2.5. Unilateral damage in a RC frame element in any aspect ratio.

3 Model Validation

The validation of the lumped damage model is performed by comparing experimental results from the literature with results obtained through numerical simulations. The experimental program used was performed by Perdomo (2010) [8] and aims to evaluate the inelastic behavior and failure mechanism of RC elements subjected to external forces. The tests were performed at the Structural Mechanics Laboratory at Lisandro Alvarado University, Venezuela.

Numerical simulations are performed using various Fortran subroutines written with the Abaqus structural analysis software processor. The parallel use of both programs is necessary for the preprocessing steps (determination of parameters associated with the mechanical properties of materials, introduction of boundary conditions, definition of the cross and longitudinal sections of each element, etc.), processing (calculations of the plasticity variables, damage, force-displacement behavior curves, etc.) and post-processing (visualization and interpretation of results, identification of the most damaged structural element) of the simulations.

3.1 Analysis of beams with different aspect ratios

To analyze the influence of shear force on the inelastic behavior of RC beams, Perdomo (2010) performed an experiment in which two specimens with different aspect ratios are subjected to monotonic lateral loading. The beams are designed based on ACI (2005) [5] specifications. The physical and geometric characteristics are shown in Table 3.1.

Table 3.1. Physical and geometric characteristics of the beams (PERDOMO, 2010 [8]).

RC Specimen	w (mm)	t (mm)	a (mm)	c_{long} (mm)	c_{trans} (mm)	d (mm)	a/d (-)	f'_c (MPa)	f_y (MPa)
B-M160	250	250	1600	25	12	225	7,11	26,7	412
B-M80	250	250	800	25	12	225	3,55	26,7	412

t = width of cross section;
w = height of cross section;
a = lateral load application point;
c_{long} = nominal coverage of longitudinal reinforcement;
c_{trans} = nominal coverage of transverse reinforcement;
f'_c = characteristic strength of concrete;
f_y = characteristic strength of steel.

The model uses two auxiliary programs named Generator 1 and Generator 2 (G1 and G2) to calculate the mechanical properties of the material and the parameters that define the inelastic behavior of RC elements. The programs G1 and G2 are composed of several subroutines implemented in Fortran language and coupled to the lumped damage model. The calculations are performed through interaction diagrams that relate axial load values to bending moments, shear forces, plastic curvatures and plastic distortions. The Fig. 3.1 presents the static schematic of the structure and the history of lateral displacement applied to the different points of the element.

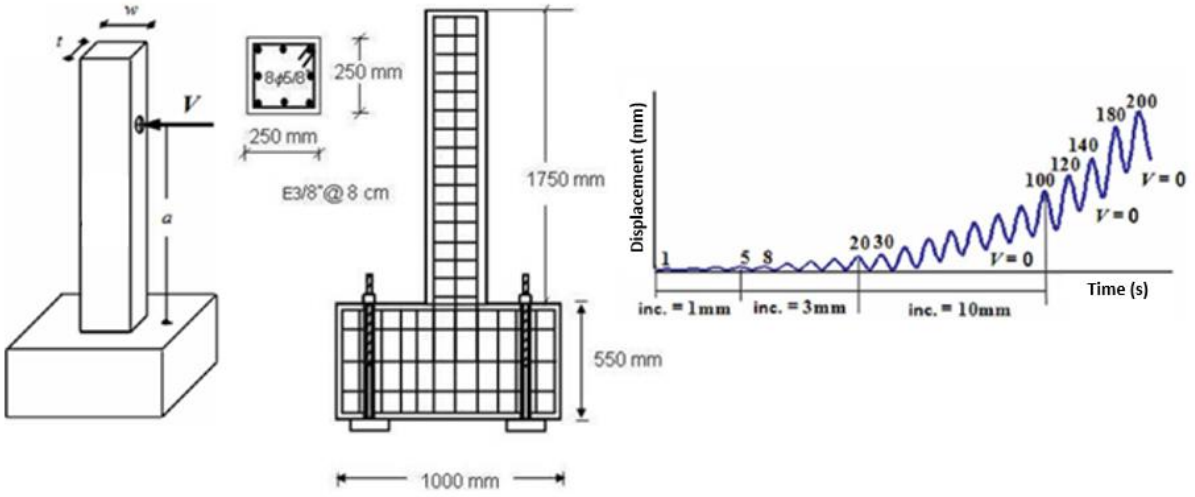

(a) Cantilever Beam (b) Monotonic displacement history

Figure 3.1. Slender beam experimentally tested by Perdomo (2010) [8].

The behavior curves (experimental and numerical) of beam B-M160 are shown in Fig. 3.2. The curve obtained by numerical simulation shows an adequate correlation with the experimental curve. However, it is appreciated that the simulation curve presents a steeper slope in the discharges when the displacement values are increased. The overlap of the curves and the evolution of the bending (d_i) and shear (d_s) damage variables are shown in Fig. 3.3.

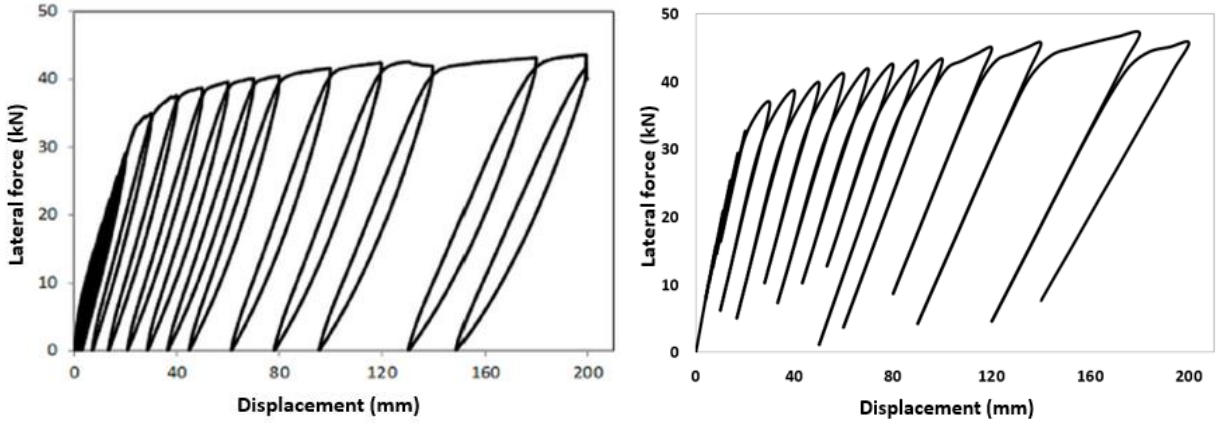

(a) Experimental result (b) Numerical simulation

Figure 3.2. Behavior curves (experimental and numerical) of beam B-M160.

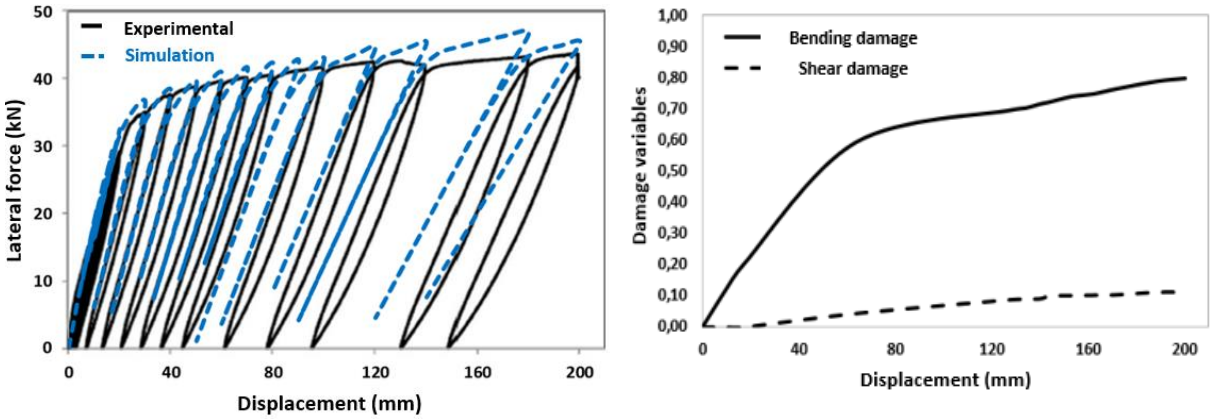

(a) Behavior curves (b) Bending and shear damage

Figure 3.3. Evolution of the damage by bending and shear in the beam B-M160.

High final values of bending damage ($d_i \approx 0{,}80$) and negligible final values of shear damage ($d_s \approx 0{,}10$) are observed, which effectively proves the minimal influence of shear deformations when the element has aspect ratio high.

The parameters that define the inelastic behavior of beam B-M80 are the same parameters calculated for beam B-M160 because only the position of load application was changed. Behavior curves (experimental and numerical) are shown in Fig. 3.4. The curve obtained through the numerical simulation (Fig. 3.4b) is satisfactory. The overlap of the behavior curves and the evolution of bending and shear damage variables are shown in Fig. 3.5.

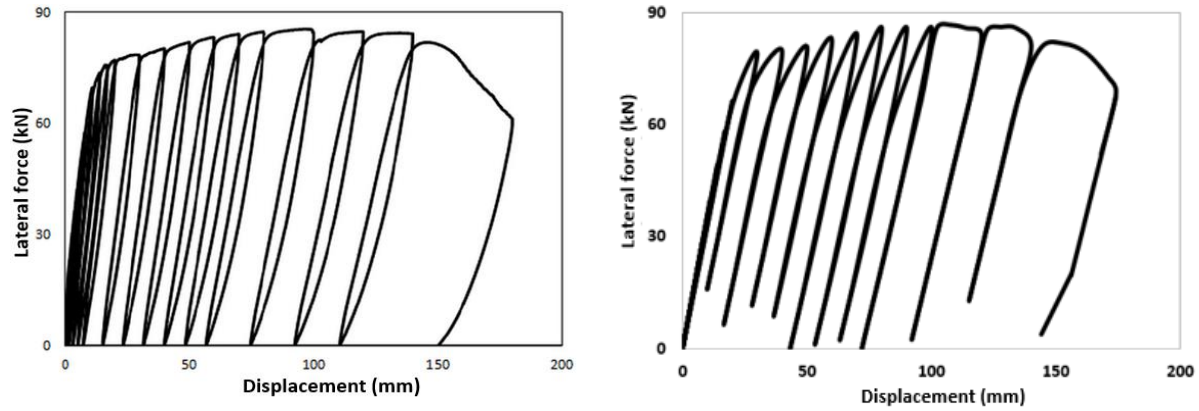

(a) Experimental result (b) Numerical simulation

Figure 3.4. Behavior curves (experimental and numerical) of beam B-M80.

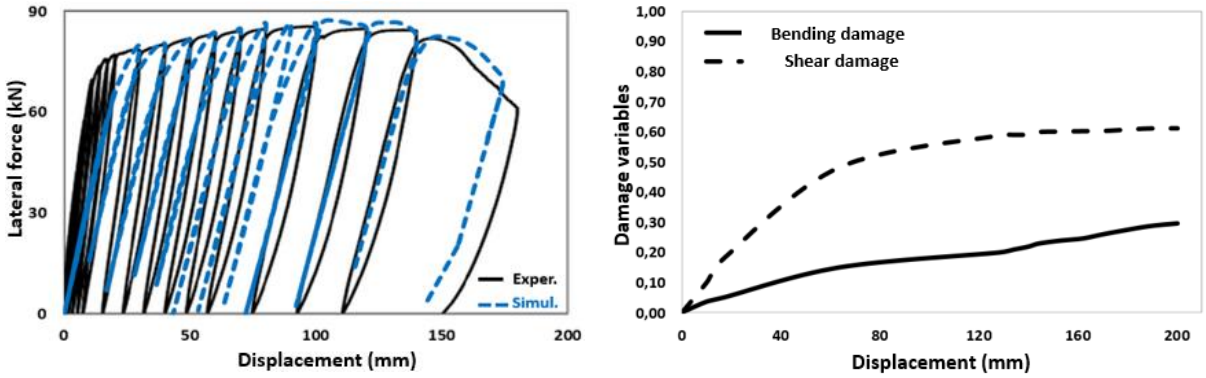

(a) Behavior curves (b) Bending and shear damage

Figure 3.5. Evolution of the damage by bending and shear in the beam B-M80.

In this case, it is observed that the final values of shear damage ($d_s \approx 0{,}62$) became higher than the final values of bending damage ($d_i \approx 0{,}25$) proving that for the analysis of short columns (i.e., elements with low aspect ratio) it is indispensable that the model to be employed is able to represent the inelastic effects induced by the combined forces of shear and bending.

3.2 Shear wall analysis SWH2

To highlight the influence of shear force on the cracking density of low aspect ratio RC elements (e.g. shear walls, short columns, etc.), Perdomo (2010) [8] also performed an experiment in which a wall is subjected to a history of cyclic loading. The shear wall SWH2 was designed based on ACI (2005) [5] specifications. The physical and geometric characteristics of the element can be seen in Table 3.2 and Figure 3.6, respectively.

Table 3.2. Physical and geometric characteristics of the shear wall SWH2 (PERDOMO, 2010 [8]).

RC Specimen	w (mm)	t (mm)	a (mm)	c_{long} (mm)	c_{trans} (mm)	d (mm)	a/d (-)	f'_c (MPa)	f_y (MPa)
SWH2	150	450	540	25	12	425	1,25	16,7	412

The behavioral (experimental and numerical) curves of the shear wall are shown in Fig. 3.7. It can be observed that the curve obtained through numerical simulation shows an adequate correlation with the experimental curve. The evolution of the bending (d_i^+, d_i^-) and shear (d_s^+, d_s^-) damage variables are shown in Fig. 3.8. It is important to mention that d_i^+ and d_i^- represent the cracking of the concrete due to the negative and positive bending moments, respectively. Variables d_s^+ and d_s^- characterize shear cracking due to negative and positive shear forces, respectively.

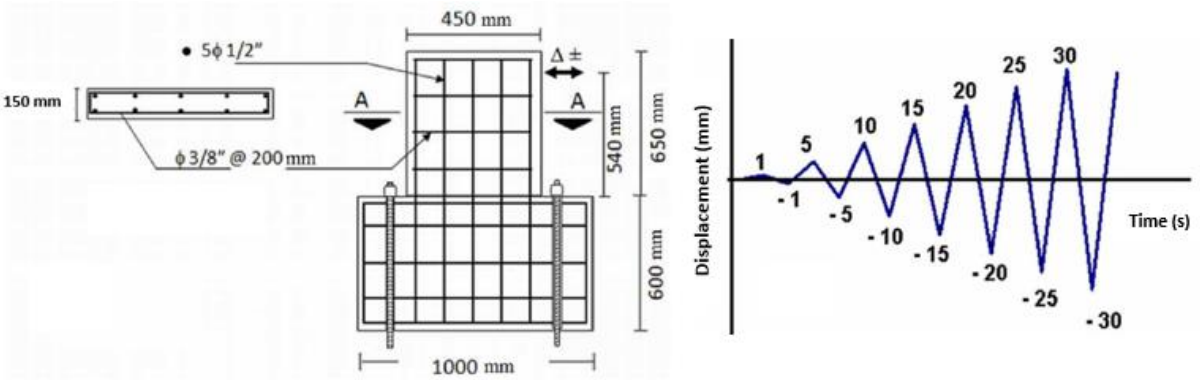

(a) Shear wall SWH2 (b) Cyclic displacement history

Figure 3.6. Shear wall experimentally tested by Perdomo (2010) [8].

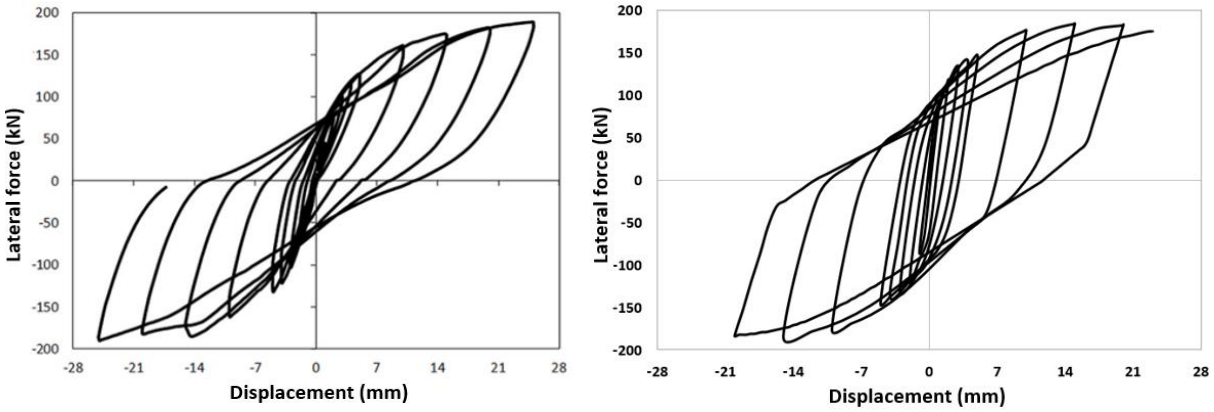

(a) Experimental result (b) Numerical simulation

Figure 3.7. Behavior curves (experimental and numerical) of shear wall SWH2.

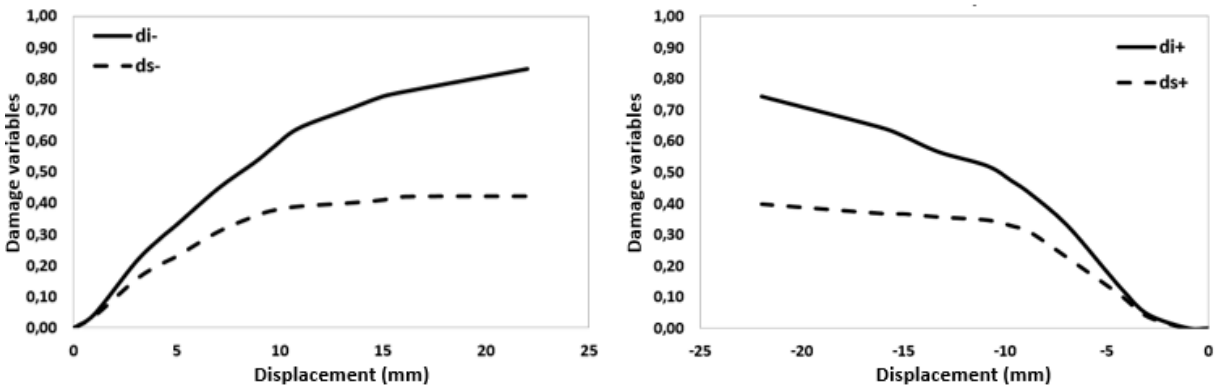

(a) Evolution of damage due to positive actions (b) Evolution of damage due to negative actions

Figure 3.8. Evolution of the damage by bending and shear in the shear wall SWH2.

High final bending damage values and not negligible final shear damage values are observed. The behavior curve and damage values show that for the diagnosis of buildings using dual systems as a structural alternative, it is essential that the model employed in the analysis be able to quantify the cracking density due to the combined effects of bending and shear.

3.3 Column analysis considering axial load effect: B-M160CA

The main objective of inelastic constitutive models is to represent as realistically as possible most of the effects that are induced on structures when subjected to external loads. In this context, the lumped damage model, in addition to considering the inelastic behavior of structures under cyclic, monotonic, static and dynamic loading, considers the inelastic effects produced by axial loading. To validate the model in this situation, a slender column (named B-M160CA) with an aspect ratio of 7.11 was simulated. The RC element, in addition to being subjected to a history of cyclic displacement, is axially loaded as shown in Fig. 3.9. The physical and geometric characteristics of the element are presented in Table 3.3.

Table 3.3. Physical and geometric characteristics of the column B-M160CA (PERDOMO, 2010 [8]).

RC Specimen	w (mm)	t (mm)	a (mm)	c_{long} (mm)	c_{trans} (mm)	d (mm)	a/d (-)	f'_c (MPa)	f_y (MPa)
B-M160CA	250	250	1600	25	12	225	7,11	26,7	412

The behavioral (experimental and numerical) curves of element B-M160CA are shown in Fig. 3.10.

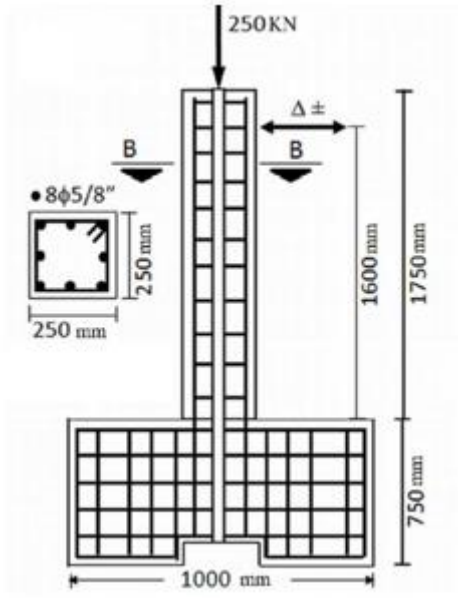

(a) Cantilever Column

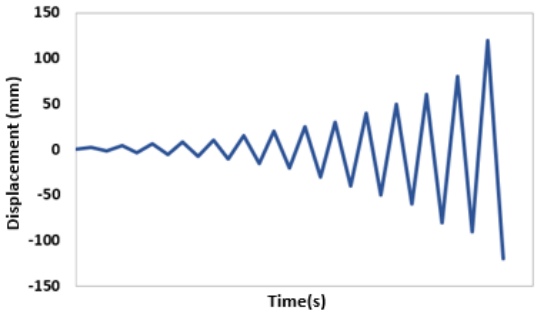

(b) Cyclic displacement history

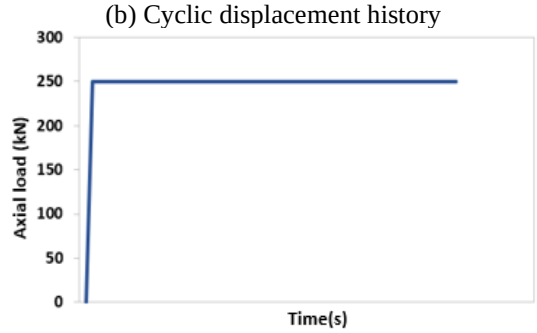

(c) Axial load

Figure 3.9. Column experimentally tested by Perdomo (2010) [8].

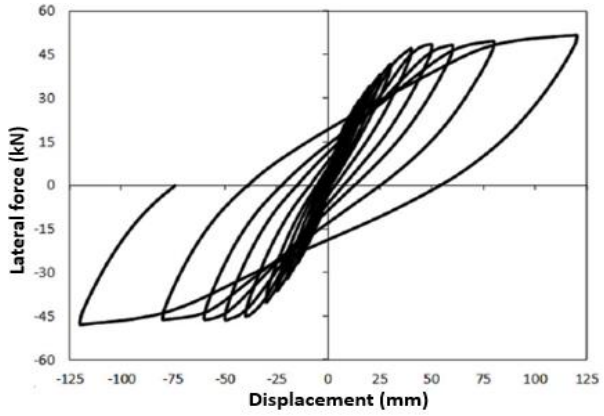

(a) Experimental result

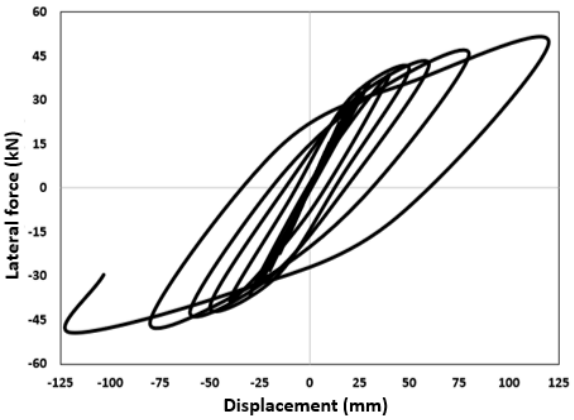

(b) Numerical simulation

Figure 3.10. Behavior curves (experimental and numerical) of column B-M160CA.

The behavior curve obtained through the simulation is acceptable. The evolution of flexural (d_i^+, d_i^-) and shear (d_s^+, d_s^-) damage variables can be seen in Fig. 3.11.

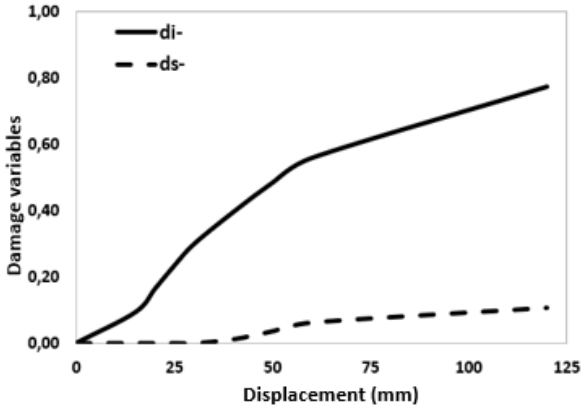

(a) Evolution of damage due to positive actions

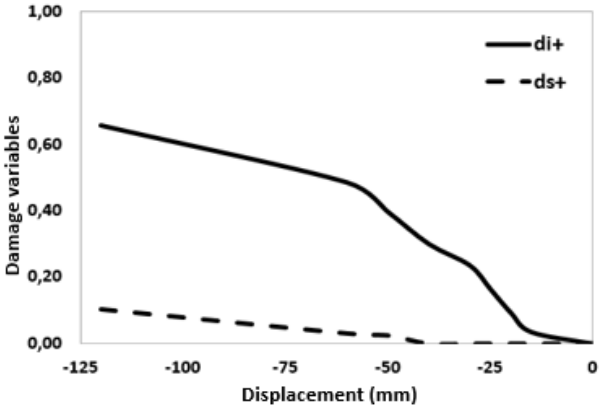

(b) Evolution of damage due to negative actions

Figure 3.11. Evolution of the damage by flexural and shear in the column B-M160CA.

Considerable bending damage values ($d_i^+ \approx 0{,}66,\ d_i^- \approx 0{,}77$) and negligible final shear damage values ($d_s^+ \approx 0{,}07,\ d_s^- \approx 0{,}09$) were obtained considering an axial load of 250kN. The behavioral curve and the damage values obtained by numerical simulation show the beneficial influence (until reaching the balanced load) of the axial load. Note that damage values may be decreased depending on the RC element confinement level.

3.4 Beam analysis considering the effect of low cycle fatigue: C160-1

Besides considering the structural behavior under cyclic, monotonic, static, dynamic loading and the inelastic effects produced by the axial load, the model also considers the inelastic behavior of the RC elements when subjected to cyclic low cycle loads. To validate the model in this situation, a slender beam (named C160-1) with an aspect ratio of 7.11 was simulated. The physical and geometric characteristics are presented in Table 3.4 and Fig. 3.12.

Table 3.4. Physical and geometric characteristics of the slender beam C160-1 (MUÑOZ, 2017 [9]).

RC Specimen	w (mm)	t (mm)	a (mm)	c_{long} (mm)	c_{trans} (mm)	d (mm)	a/d (-)	f'_c (MPa)	f_y (MPa)
C160-1	250	250	1600	25	12	225	7,11	23,5	412

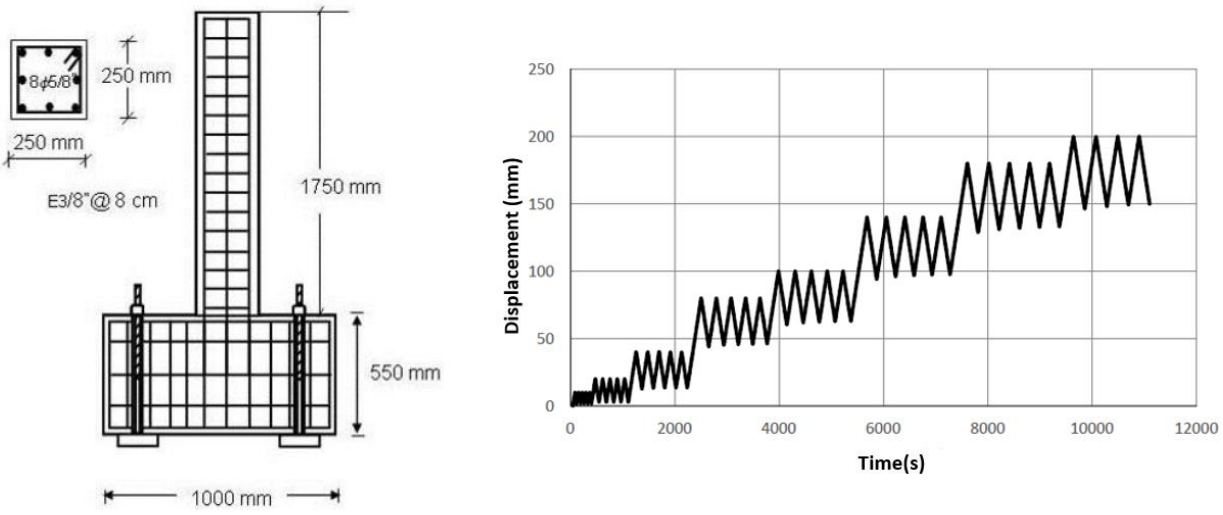

(a) Cantilever Beam (b) Displacement history

Figure 3.12. Slender beam experimentally tested by Muñoz (2017) [9].

Behavior curves (experimental and numerical) are shown in Fig. 3.13. The curve obtained through numerical simulation (see Fig. 3.13b) is acceptable. The overlap of the behavior curves and the evolution bending damage variable are shown in Fig. 3.14.

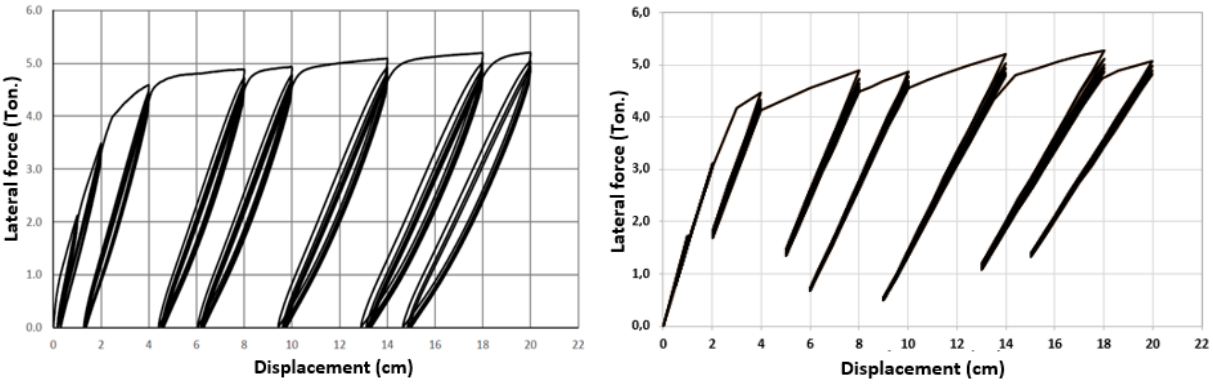

(a) Experimental result (b) Numerical simulation

Figure 3.13. Behavior curves (experimental and numerical) of slender beam C160-1.

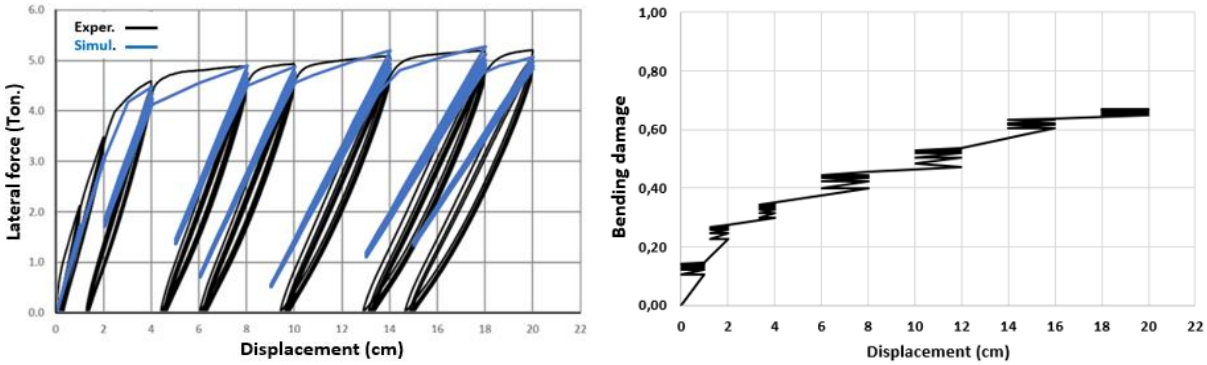

(a) Behavior curves (b) Evolution of bending damage

Figure 3.14. Evolution of the damage by slender beam C160-1.

The final value of the bending damage was 0,67 and the final value of the damage per shear was 0,12. The behavior curves (experimental and numerical) and evolution curve of the bending damage (Fig. 3.14b) shows the loss of rigidity of the material due to the effect of low cycle fatigue demonstrating that the lumped damage model is also capable of representing this phenomenon.

4 Simulation of a dual system considering the El Centro Earthquake

Analyzing the inelastic response of dual systems when subjected to seismic accelerations is of great relevance in structural engineering because, according to the behavior obtained, it is possible to formulate mitigation measures to prevent collapse and maintain the structural integrity of buildings. In this context, a simulation was carried out in which the acceleration values produced by the El Centro Earthquake recorded in 1940 in southeastern Southern California, near the international border of the United States and Mexico. The El Centro Earthquake presented a magnitude of momentum of 6.9 and a maximum intensity perceived in the Mercalli intensity scale. The acceleration history used lasts approximately 25 seconds.

The physical and geometric characteristics of the structure are detailed in Table 4.1 and Fig. 4.1, respectively.

Table 4.1. Physical and geometric characteristics of the dual system (NEUMANN, 2018 [10]).

Structure of RC	**Element type of RC**	***w*** **(mm)**	***t*** **(mm)**	***a*** **(mm)**	c_{long} **(mm)**	c_{trans} **(mm)**	***d*** **(mm)**	***a/d*** **(-)**	f'_c **(MPa)**	f_y **(MPa)**
PDS1	Shear wall	250	1000	1475	25	12,25	950	1,51	16,7	420
	Slender beam	250	250	1475	25	12,00	225	6,55	16,7	420

The history of accelerations is shown in Fig. 4.2 and the history of displacements obtained through the simulation is shown in Fig. 4.3. The final damage values are shown in Fig. 4.4. It is important to mention that d_i^+ and d_i^- represent the cracking of the concrete due to the negative and positive bending moments, respectively. Variables d_s^+ and d_s^- characterize shear cracking due to negative and positive shear forces, respectively.

Once the structure behavior is determined and damage values are calculated, the results are verified using certain acceptance criteria. These criteria, in general, will consider the seismic performance of the structure and the levels of damage presented after the seismic event. More details on the acceptance criteria and the diagnosis of structural vulnerability can be found in Flórez-López et. al, (2014) [1].

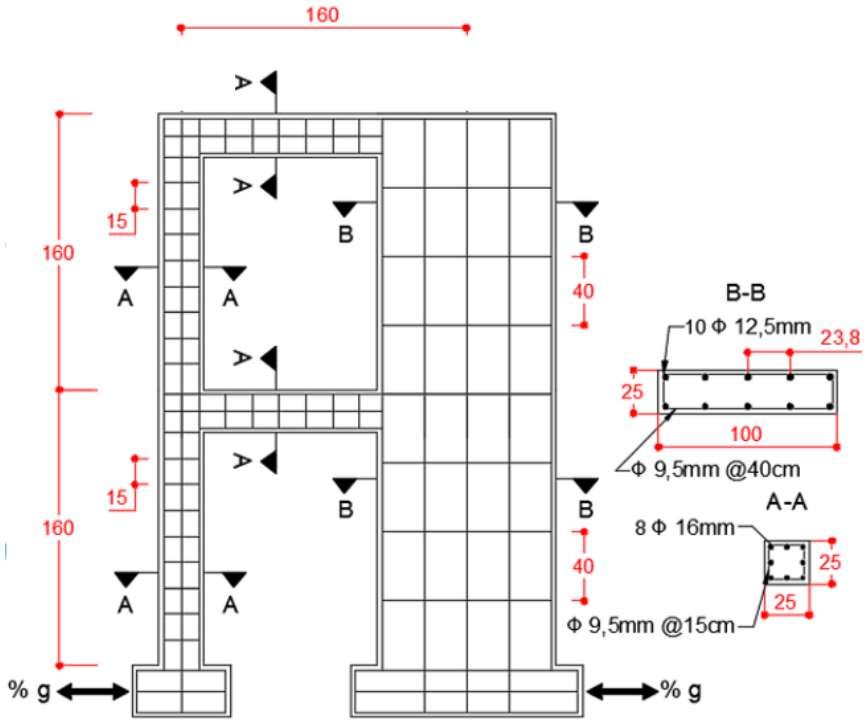

Figure 4.1. Dual system details (dimensions in centimeters).

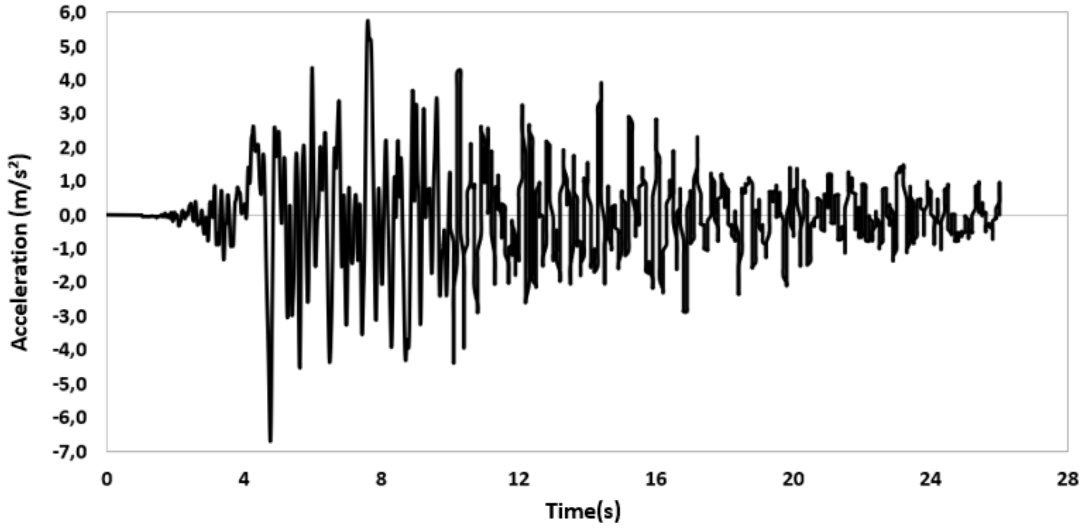

Figure 4.2. Acceleration history of El Centro Earthquake.

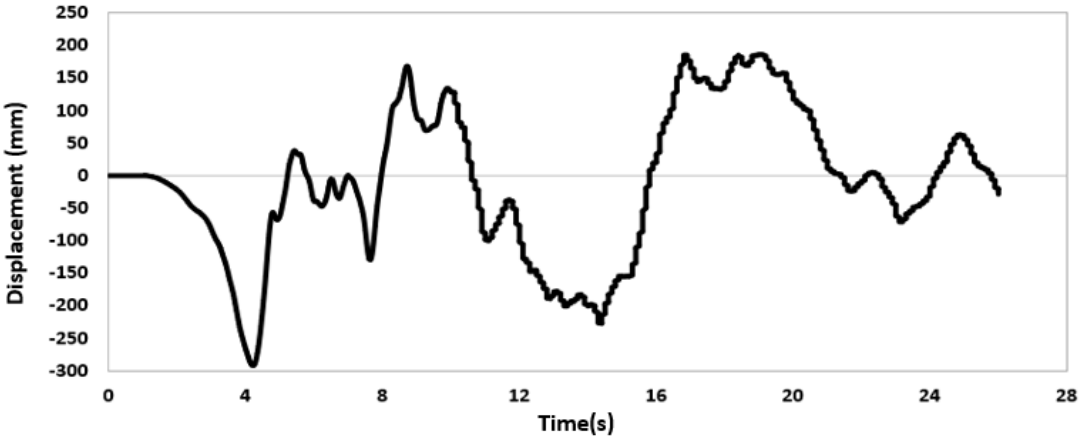

Figure 4.3. History of displacements obtained through the simulation.

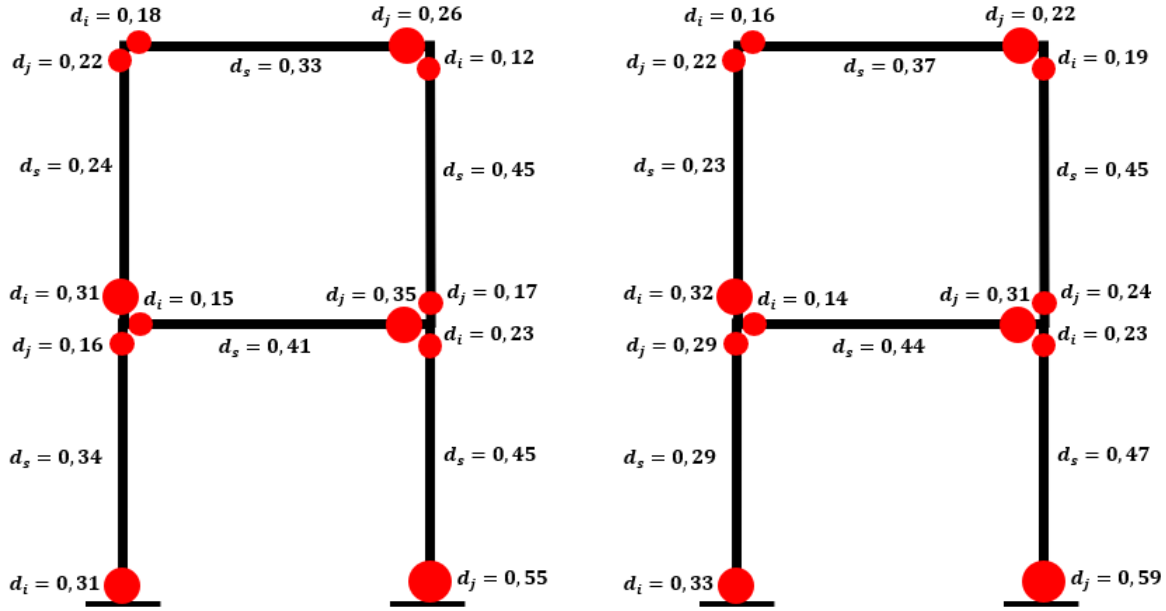

(a) Positive damage variables (b) Negative damage variables

Figure 4.4. Final values of damage by bending and shear in the PDS1 structure.

5 Conclusions

In this paper, a behavior model based on lumped damage mechanics was presented to determine the inelastic behavior of buildings using dual systems as a structural alternative. The model is capable of describing the concrete cracking process, quantifying the plastic deformations of longitudinal and transverse reinforcement and predicting the loss of structural element stiffness by varying the inclinations in the discharges observed through the force-displacement curves. The model can be used for the diagnosis of buildings that were subjected to seismic loads and that present structural elements with varied aspect ratios.

Acknowledgements

This work arose through scientific initiation projects carried out at the Federal University of Latin American Integration. The first author thanks the Institutional Program of Scientific Initiation - PIBIC for the financing provided. We also thank Maria Elena Perdomo and Maria Fabiana Muñoz for making available the experimental program data, indispensable for the validation of lumped damage model.

References

[1] FLÓREZ-LÓPEZ, J; MARANTE, M. E; PICÓN, R. **Fracture and Damage Mechanics for Structural Engineering of Frames**: state-of the-art industrial applications. United States of America: Engineering Science Reference (an Imprint of Igi Global), 2014.

[2] PERDOMO, M. E.; PICÓN, R; MARANTE, M. E; HILD, F; ROUX, S; FLÓREZ-LÓPEZ, J. Experimental analysis and mathematical modeling of fracture in RC elements with any aspect ratio. **Engineering Structures**, v. 46, p.407-416. 2013. Elsevier BV. http://dx.doi.org/10.1016/j.engstruct.2012.07.005.

[3] THOMSON, E; PERDOMO, M. E.; PICÓN, R; MARANTE, M. E; FLÓREZ-LÓPEZ, J. Simplified model for damage in squat RC shear walls. **Engineering Structures**, v. 31, n. 10, p.2215-2223, out. 2009. Elsevier BV. http://dx.doi.org/10.1016/j.engstruct.2009.05.020.

[4] LEMAITRE, L; CHABOCHE J. L. **Mechanics of solids materials.** Paris: Dunod, 1998.

[5] AMERICAN CONCRETE INSTITUTE. Building code requirement for structural concrete. ACI Committee 318, Farmington Hills, Mich.; 2005.
[6] SEZEN, H; MOEHLE, J. P. Seismic behavior and modeling of reinforced concrete building columns. **Journal of Structural Engineering Asce**, University of Michigan, p.130-142, out. 2004.
[7] CIPOLLINA, A; LÓPEZ-INOJOSA, A; FLÓREZ-LÓPEZ, J. A simplified damage mechanics approach to nonlinear analysis of frames. **Elsevier**: Computers & Structures, U.s, p.13-26. 1995.
[8] PERDOMO, M. E. **Fractura y Daño en Estructuras Duales de Concreto Armado.** 340 f. Tese (Doutorado) - Curso de Doctorado En Ciencias Aplicadas, Facultad de Ingenieria, Universidad de Los Andes, Mérida, Venezuela, 2010.
[9] MUÑOZ, M. F. **Aportes al modelo histerético de daño con fatiga de bajo ciclaje en elementos de concreto armado para fallas dominantes a corte y flexión.** 122 f. Dissertação, Dirección de Postgrado - Maestría En Mecánica Aplicada a la Construcción, Universidad Centroccidental "Lisandro Alvarado", Barquisimeto, Venezuela, 2017.
[10] NEUMANN, J. **Análise de fissuração em estruturas duais de concreto armado através de simulações numéricas baseadas na mecânica do dano.** TCC (Graduação) - Curso de Engenharia Civil de Infraestrutura, Instituto Latino-americano de Tecnologia, Infraestrutura e Território, Universidade Federal da Integração Latino-americana, Foz do Iguacu, 2018.
[11] MAZARS, J; BERTHAUD, Y; RAMTANI, S. The unilateral behavior of damaged concrete, **Engng. Fract. Mech**. 629–635, 1990.
[12] LADEVÈZE, P. **Mechanics and mechanisms of damage in composites and multimaterials**, in: D. Baptiste (Ed.), MEP, London, 1991.